

Article

Investigation of Co_3O_4 and LaCoO_3 Interaction by Performing N_2O Decomposition Tests under Co_3O_4 - CoO Transition Temperature

Ewa M. Iwanek (nee Wilczkowska)^{1,2,*}, Leonarda F. Liotta^{3,*} , Giuseppe Pantaleo³ , Krzysztof Krawczyk², Ewa Gdya², Jan Petryk², Janusz W. Sobczak⁴  and Zbigniew Kaszukur⁴ 

¹ Faculty of Applied Science and Technology, Sheridan College, Brampton, ON L6Y 5H9, Canada

² Faculty of Chemistry, Warsaw University of Technology, 00-664 Warsaw, Poland; kraw@ch.pw.edu.pl (K.K.); e.m.stepien@o2.pl (E.G.); jmpetryk@ch.pw.edu.pl (J.P.)

³ Istituto per lo Studio di Materiali Nanostrutturati (ISMN)-CNR, Via Ugo La Malfa, 153, I-90146 Palermo, Italy; giuseppe-pantaleo@cnr.it

⁴ Institute of Physical Chemistry, Polish Academy of Sciences, 01-224 Warsaw, Poland; jsobczak@ichf.edu.pl (J.W.S.); zkaszukur@ichf.edu.pl (Z.K.)

* Correspondence: ewa.iwanek@sheridancollege.ca (E.M.I.); leonardafrancesca.liotta@cnr.it (L.F.L.)

Abstract: The research presented in this paper addresses the question: How does the addition of a small amount of LaCoO_3 impact the activity of a Co_3O_4 catalyst? By testing such a catalyst in N_2O decomposition under conditions at which the thermal decomposition of Co_3O_4 to CoO is possible, one gains unique insight into how the two phases interact. The activity of such a catalyst increases in the entire studied temperature range, unlike the activity of the undoped cobalt catalyst which is lower at 850 °C than at 800 °C due to the reduction of Co_3O_4 to CoO . XRD measurements showed that CoO was also the main cobalt oxide present in the $\text{Co}_3.5\text{La}$ catalyst after operating at 850 °C, as did the XPS measurements, but there was no drop of activity associated with this change. The influence of NO , O_2 and H_2O on the activity of the new catalyst, $\text{Co}_3.5\text{La}$, was determined. Lack of positive effect of NO , a known oxygen scavenger, on the activity was noticed at all temperatures, showing that the effect of LaCoO_3 is probably due to increased oxygen desorption. Temperature programmed oxidation (TPO) tests showed that the beneficial effects of the presence of LaCoO_3 on the activity of cobalt oxide at 850 °C were probably caused by enhanced diffusion of O^{2-} anions through the entire catalyst, which facilitates desorption of oxygen molecules from the surface.

Keywords: nitrous oxide decomposition; cobalt-based catalysts; LaCoO_3 ; nitric oxide; water vapor



Citation: Iwanek (nee Wilczkowska), E.M.; Liotta, L.F.; Pantaleo, G.; Krawczyk, K.; Gdya, E.; Petryk, J.; Sobczak, J.W.; Kaszukur, Z. Investigation of Co_3O_4 and LaCoO_3 Interaction by Performing N_2O Decomposition Tests under Co_3O_4 - CoO Transition Temperature. *Catalysts* **2021**, *11*, 325. <https://doi.org/10.3390/catal11030325>

Academic Editor: Lucie Obalová

Received: 6 February 2021

Accepted: 27 February 2021

Published: 4 March 2021

Publisher's Note: MDPI stays neutral with regard to jurisdictional claims in published maps and institutional affiliations.



Copyright: © 2021 by the authors. Licensee MDPI, Basel, Switzerland. This article is an open access article distributed under the terms and conditions of the Creative Commons Attribution (CC BY) license (<https://creativecommons.org/licenses/by/4.0/>).

1. Introduction

Cobalt oxides, especially Co_3O_4 , continue to be of interest to scientists from different disciplines due to the effective redox properties of this compound ([1] and references therein). Co_3O_4 is one of the catalysts still currently studied in deNO_x reactions [2,3]. As a catalyst, Co_3O_4 is commonly promoted with other oxides, such as ceria [4–9] and lanthanum cobaltate [10–13]. Studies on the cobalt catalyst doped with CeO_2 [4–9] show a beneficial effect of this compound on the activity in high-temperature decomposition of N_2O , as well as combustion of propene, methane and toluene, even though ceria alone does not catalyze these reactions. Cerium oxide, especially when doped with gadolinium, is a solid electrolyte applied in solid oxide fuel cell (SOFC) applications [14–16] because of its high ionic conductivity. However, the limitations of ceria in SOFCs are due to the fact that at high temperatures or low oxygen partial pressures ceria exhibits mixed ionic and electronic conductivity [17]. On the other hand, perovskite type oxides conduct only ions, and compounds such as lanthanum cobaltate, LaCoO_3 (LCO), are often used in SOFCs as the cathode material [18–20].

Previously performed studies on Co_3O_4 - LaCoO_3 systems have shown that even a small amount of lanthanum cobaltate has a substantial impact on the properties and hence on the catalytic activity of the obtained system in propene combustion [11]. Therefore, in the current study, the activity of a cobalt catalyst containing 3.5 mol % of lanthanum (3.5 mol % = mol La/(mol La + mol Co)) in the form of LaCoO_3 , which exhibits the perovskite structure, is investigated. The novelty of the present work is probing the interaction between Co_3O_4 and LaCoO_3 further, this time in a different reaction (N_2O decomposition), at a temperature at which the thermal reduction of Co_3O_4 is possible, as well as using both characterization studies and the addition of probe molecules in the inlet stream to gain insight into this interaction. In order to mitigate the impact of the perovskite addition on the surface area [11] and to avoid any additional sintering during the high temperature activity tests, the catalysts were exposed to prolonged treatment at 850 °C, as in the case of our previously studied series of Ce_xCo catalysts for nitrous oxide decomposition [5]. Lanthanum cobaltate is stable at high temperatures and also known for high conductivity [21–23]. Extensive characterization studies, including XPS, XRD, nitrogen physisorption, SEM imaging and Temperature Programmed Oxidation (TPO) measurements, have been performed in order to attempt to explain the impact of LaCoO_3 .

The decomposition of nitrous oxide, whose main industrial source is nitric acid plants, continues to be a topic investigated by several research groups [24–26]. Catalytic decomposition seems to be the best available solution and preferably as a second stage directly downstream of the platinum–rhodium gauze in the high-temperature zone [25,27]. It has been reported in literature that the activity of catalysts for the decomposition of nitrous oxide is reduced by the addition of water vapor to the reaction mixture [28–30]. The influence of water vapor on the N_2O conversion rates was tested on various types of catalysts [31]. The water vapor content most commonly used in experiments is 5 or 10 vol %. The presence of water vapor in the reaction mixture is known to cause a decrease of the activity of the nitrous oxide decomposition catalysts regardless of the temperature of the reaction [32–36]. The negative impact of water vapor on the activity in the decomposition of N_2O was also found in the presence of the undoped cobalt catalyst in the temperatures range: 700–850 °C [37]. In contrast, the opinion on the effect of nitric oxide is not univocal. A negative effect of nitric oxide on the activity in nitrous oxide decomposition has been noted on catalysts consisting of noble metals on supports, mixed oxides of nickel or copper obtained from hydrotalcite-type anionic clays [29], Fe_2O_3 supported on alumina [38], Co-MgO [39] and catalysts containing CeO_2 and Co_3O_4 with high Ce/Co ratios [40]. However, in the case of various types of zeolite catalysts a positive effect of nitric oxide (II) in the inlet stream on nitrous oxide decomposition was observed [41–43]. The beneficial effect of the presence of nitric oxide on the activity of the undoped cobalt catalyst was observed at 850 °C [37]. It was stated that the effect probably results from the impact of NO on the N_2O decomposition mechanism, i.e., a scavenger effect, not the state of the catalyst [37].

2. Results and Discussion

Figure 1 contains a schematic of the preparation of the catalyst which contains 3.5 mol % La as calculated using Equation 1. Due to the fact that lanthanum oxide is highly hygroscopic, it was dried prior to use. Afterwards, nitric acid was added to the oxide, so that the Co_3O_4 would be impregnated with a solution of lanthanum nitrate. The nitrate was then decomposed to lanthanum oxide (Figure 1), which then reacted with some of the Co_3O_4 to form lanthanum cobaltate. The X-ray diffraction pattern of the fresh catalyst confirmed that the reaction consumed all of the available lanthanum oxide (Figure 2). It revealed the presence of signals from two phases, namely, Co_3O_4 and LaCoO_3 . The following reference diffraction patterns of the catalyst are shown below for clarity: Co_3O_4 (71-0816) and LaCoO_3 (48-0123). The XRD results show that both phases have crystallites with the average size above 100nm before and after the catalytic tests due to the prolonged high-temperature treatment during the synthesis (Figure 1).

$$C_{\text{La}} = [n_{\text{La}} / (n_{\text{La}} + n_{\text{Co}})] \cdot 100 \quad (1)$$

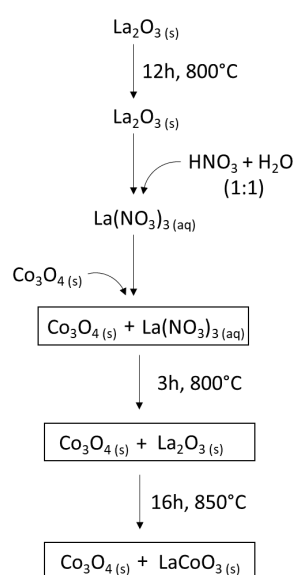


Figure 1. Scheme showing the synthesis of Co3.5La.

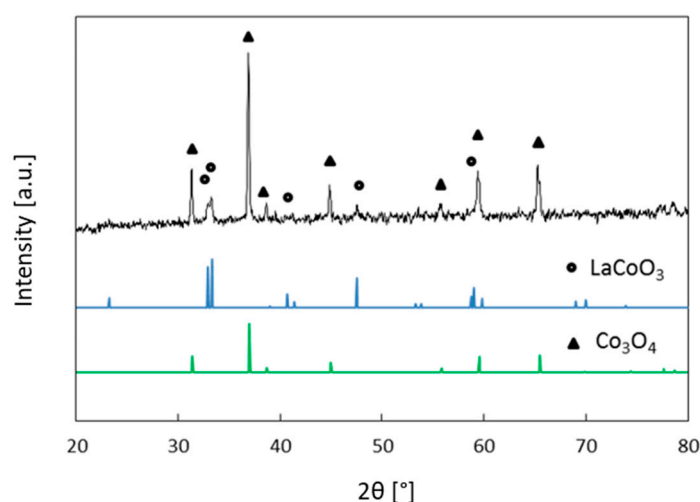


Figure 2. The X-ray diffraction (XRD) pattern of Co3.5La before experiments along with the appropriate reference patterns of LaCoO₃ (48-0123)—circles and Co₃O₄ (71-0816)—triangles.

The nitrogen physisorption measurements revealed that the surface of the lanthanum-doped cobalt catalyst and that of the undoped cobalt catalyst is very small, not exceeding $2\text{m}^2\cdot\text{g}^{-1}$, i.e., 1.78 and $0.63\text{m}^2\cdot\text{g}^{-1}$, respectively. Moreover, both values slightly decrease to around $0.5\text{m}^2\cdot\text{g}^{-1}$ during operation in the reactor. Figure 3a shows the pore size distribution of the fresh catalyst in comparison to that of undoped Co₃O₄. A similar distribution was found in both cases. The SEM images of Co3.5La before and after catalytic tests can be seen in Figure 3b,c, respectively. The morphology of both samples is comparable.

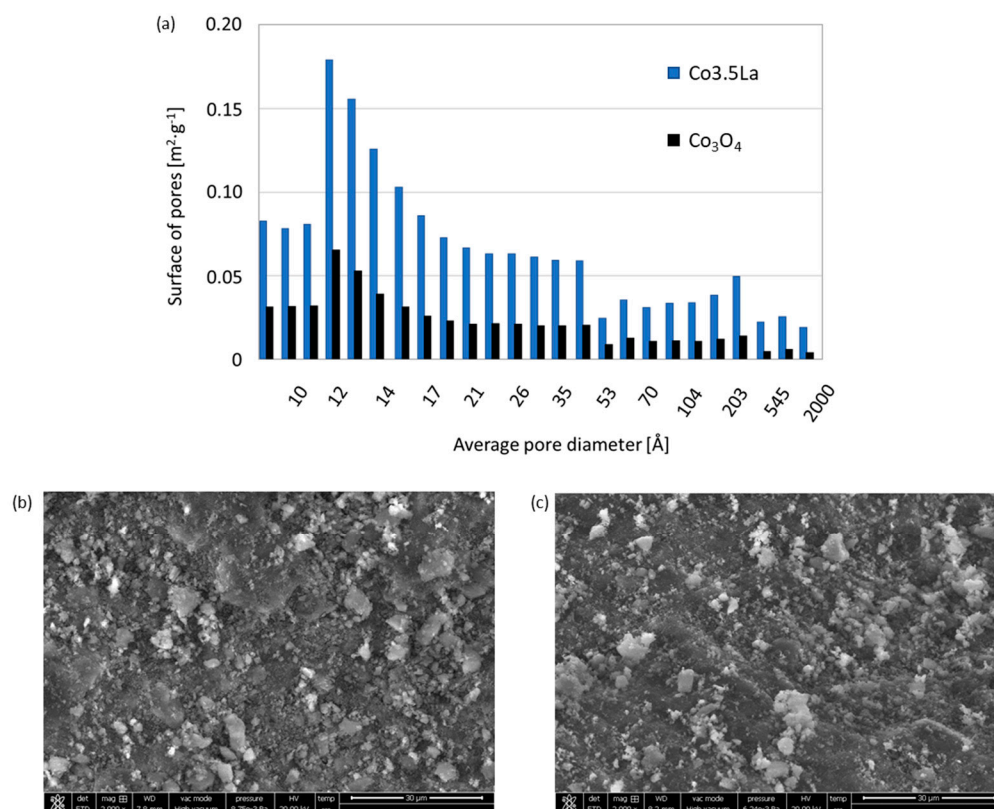


Figure 3. Results of characterization studies: (a) porosimetry test results for the fresh undoped cobalt catalyst (black) and $\text{Co}_{3.5}\text{La}$ (blue) and SEM images of $\text{Co}_{3.5}\text{La}$ (b) fresh and (c) after catalytic tests.

From previously performed studies of the undoped cobalt catalyst and Co-Ce systems [5], it is known that two factors affect the performance of cobalt-based systems in the studied reaction at high temperatures. First of all, it is the oxidation state of cobalt in the oxide. At 850°C CoO dominates, which leads to lower N_2O conversions. At 850°C after the addition of 5 vol % O_2 to the inlet stream, Co_3O_4 is the dominant cobalt oxide, which leads to higher N_2O conversions than in an inlet stream without oxygen in the case of the undoped cobalt oxide as shown in [5]. The second parameter which influences N_2O conversion is the Rate Determining Step (RDS) of the reaction, namely desorption of molecular oxygen, which can be improved by the addition of NO to the inlet mixture.

The Mars van Krevelen mechanism, which is typically used to describe oxidation, is composed of the following steps (CO oxidation is used as an example):

- (1) adsorption of an oxygen molecule on the surface of the catalyst (filling two anion vacancies) and adsorption of two CO molecules by the oxygen atom,
- (2) reaction of each CO molecule with an oxygen anion,
- (3) desorption of two molecules of CO_2 with the regeneration of the oxygen ion vacancies on the surface.

In the case of the decomposition of nitrous oxide, the following steps occur:

- (1) adsorption of a N_2O molecule by the oxygen atom on the catalyst surface,
- (2) cleavage of the N-O bond and departure of N_2 , leaving an oxygen anion on the surface of the catalyst,
- (3) adsorption of another N_2O molecule directly onto a surface oxygen anion to form N_2 and O_2 (Eley-Rideal mechanism), or onto another spot, cleavage of the N-O bond and subsequent migration of oxygen anions to form an O_2 molecule (Langmuir-Hinshelwood mechanism)
- (4) desorption of oxygen from the surface of the catalyst (rate determining step [6]).

From the point of the catalytic systems, in both types of reactions, a redox cycle occurs. In the case of CO oxidation (see [44] and Figure 3) a cobalt ion in an octahedral site with unsaturated coordination is the active site. It is possible that the redox cycle in N₂O decomposition also occurs on this site. The electron transfer from the catalyst to either CO or N₂O molecule occurs, and a vacancy on the catalyst surface is filled. This is followed by the formation of a bond between an oxygen anion on the surface and either the adsorbed CO or the oxygen anion left after the N-O bond cleavage. In both cases, an additional oxygen anion is needed to form CO₂ or O₂, respectively. Finally, electron density is transferred back to the catalyst surface when carbon dioxide or, in the case of N₂O decomposition, molecular oxygen, desorbs from the surface and the oxygen vacancy is restored.

At 850 °C the addition of NO does not change the oxidation state of cobalt, but it is known for its “oxygen scavenger” properties which facilitate the regeneration of the anion vacancies on the catalyst surface by removing the oxygen anions from the surface. The facilitation of the RDS of N₂O decomposition is the reason for its favorable influence on the activity of the undoped cobalt catalyst [37]. Similarly, the evolution of oxygen, and hence regeneration of the original adsorption site, can be improved by the addition of potassium to Co₃O₄, as reported by Asano et al. [45].

Figure 4a shows the N₂O conversion on the studied catalyst (blue bars) in the inlet stream with the composition 5 vol % N₂O in Ar in comparison with the results obtained under the same conditions for the undoped cobalt catalyst (grey bars). It can be seen that at temperatures of 700 and 750 °C, the undoped cobalt catalyst exhibits an activity that is similar to that of the catalyst containing LaCoO₃. At 800 °C the activity of both catalysts is the same. In contrast, at the highest temperature, i.e., 850 °C, the Co_{3.5}La is significantly more active than the undoped catalyst. Two recent interesting studies on high temperature N₂O decomposition have shown the significance of parameters such as extrudate size [25] and pressure [27] on N₂O decomposition. In fact, in measurements carried out at 890 °C with the commercial catalyst [25] it was found that an increase of diameter of the extrudates leads to a decrease of conversions of N₂O from approx. 80% for 2 mm diameter to 60% for 5 mm extrudates. Experiments carried out on monoliths in the temperature region 700–900 °C [27] show that the conversion of N₂O increases substantially not only with the increase in temperature, but with increase of pressure in the regime which is currently found in nitric acid plants. For the lowest studied pressure, the following N₂O conversions were obtained for 700 °C, 800 °C and 900 °C: 10%, 30% and 65%, but at 900 °C it can reach to over 90% for the highest studied pressure [27].

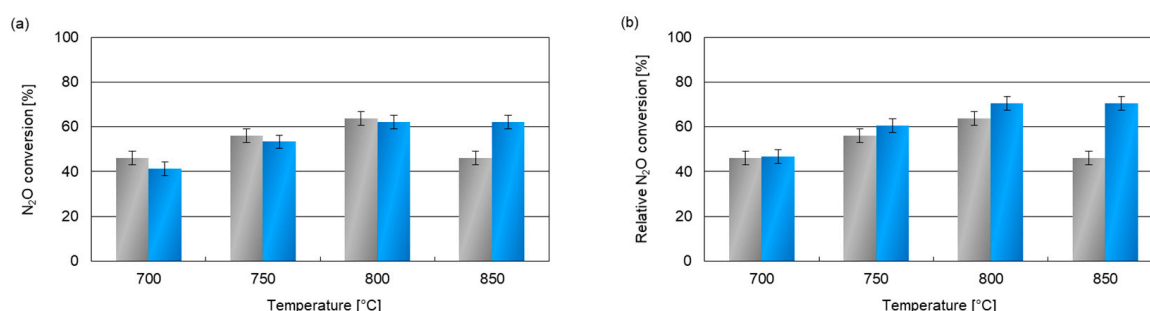


Figure 4. Nitrous oxide conversions in a stream composed of 5% N₂O in Ar on the Co_{3.5}La system (blue columns) and the undoped cobalt catalyst (grey columns): (a) conversion without accounting for difference in mass of Co₃O₄ in catalyst bed, (b) conversion relative to the mass percentage of Co₃O₄ in fresh catalyst bed.

The N₂O conversion related to the Co₃O₄ content in the fresh catalyst bed is presented in Figure 4b. The activity at the lowest temperatures is the same on both catalysts. This might indicate that the active phase in Co_{3.5}La is the spinel phase. At 750 and 800 °C the activity is similar or slightly higher in the case of Co_{3.5}La. At 850 °C, a pronounced difference is even more visible. The conversion obtained on Co_{3.5}La is higher than that

obtained on the undoped cobalt catalyst. The results noted for the two higher temperatures are the same as those observed when oxygen is added to the inlet stream introduced onto the undoped cobalt catalyst [37].

Summing up the results of activity in an inlet stream composed of 5 vol % N_2O in Ar, it should be emphasized that the catalytic activity of $\text{Co}_3.5\text{La}$ does not exhibit a decrease in activity at 850°C (Figure 4). In the case of the undoped cobalt catalyst a drop in the activity occurs at 850°C and is a consequence of the thermal decomposition of Co_3O_4 to CoO [46]. The addition of oxygen to the inlet stream shifts the temperature of the thermal decomposition of Co_3O_4 to higher values, which is why the undoped cobalt catalyst exhibits higher N_2O conversions in a stream with the composition: 5 vol % N_2O + 5 vol % O_2 in Ar [37]. Therefore, the next step was to check if the positive effect of LaCoO_3 on the activity of $\text{Co}_3.5\text{La}$ at 800°C is a result of its effect on the oxidation state of cobalt in the cobalt oxide.

Co_3O_4 is a mixed oxide and contains cobalt ions on two oxidation states, namely +2 and +3. The only type of cobalt ions present in CoO are Co^{2+} ions. In contrast cobalt in LaCoO_3 is present solely as Co^{3+} . From literature it is known that the Co 2p regions of the XPS spectra of Co^{2+} and Co^{3+} ions differ considerably. In the case of ions in the lower oxidation state intensive shake-up satellites located approximately 5.4 eV [47] to 6.3 eV [48] away from the main signals are visible in the spectrum. In the spectrum of cobalt +3, the satellites are far less intense and more distant from the main signals, by about 9–10 eV [48,49]. Figure 5 shows the Co 2p region of $\text{Co}_3.5\text{La}$ and the undoped cobalt catalyst [5] after operating at 850°C in the inlet stream: 5 vol % N_2O in Ar. In the case of the undoped catalyst (Figure 5 spectrum 1), the obtained spectrum is characteristic of the Co^{2+} ions. Thus, cobalt is present in the form of CoO . In the spectrum of the catalyst containing LaCoO_3 (Figure 5 spectrum 2) operating at 850°C in an inlet stream consisting only of nitrous oxide in an inert gas (Ar), similar satellites can be seen, which are intense and distant by about 6 eV from the main signals. Due to the presence of Co^{3+} ions in the lanthanum cobaltate, which does not undergo changes under these conditions, one can expect a very small signal corresponding to Co^{3+} ions in the Co 2p region of the spectrum of $\text{Co}_3.5\text{La}$, even at a total reduction of Co_3O_4 to CoO . As seen in Figure 5, line 2 there is a small contribution from a Co^{3+} satellite, which shows that on the surface Co_3O_4 is decomposed to CoO , as is the case of the undoped cobalt catalyst. The transformation of Co_3O_4 to CoO was also confirmed by an XRD study.

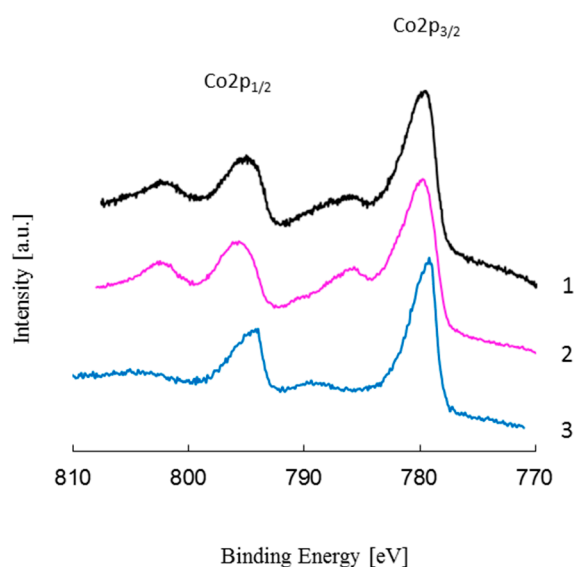


Figure 5. Results of XPS measurements: the Co 2p region of the undoped cobalt catalyst and $\text{Co}_3.5\text{La}$ after tests in a stream with the inlet composition: 5% N_2O + 95% Ar (1 and 2, respectively) and $\text{Co}_3.5\text{La}$ after tests in stream with inlet composition 5% N_2O + 5% O_2 + 90%Ar (3).

The results of the XPS studies are in line with the conclusions drawn on the thermodynamic calculations. They clearly show that the presence of LaCoO_3 in the catalytic system does not influence the oxidation state of cobalt in the oxide in streams with the following inlet compositions: 5 vol % N_2O + 95 vol % Ar and 5 vol % N_2O + 5 vol % O_2 + 90 vol % Ar (Figure 5 spectrum 3) because it is the same as in the undoped cobalt catalyst [37]. Summing up this part of the study, it can be concluded that the positive effect of lanthanum on the catalyst activity at 850 °C does not result from the impact of LaCoO_3 on the oxidation state of cobalt.

Figure 6 summarizes the results of activity tests carried out on the cobalt catalyst containing lanthanum in streams with various composition. Figure 6a shows the effect of oxygen concentration in the inlet stream on N_2O conversion. It can be seen that there is a negative effect of the additional oxygen on the activity of the catalyst, except at 850 °C, at which there is a slight increase of the N_2O conversion, which is probably due to the fact that more cobalt is in the Co_3O_4 form, as indicated in the XPS results. Such a theory can be verified by XRD studies of the bulk composition of the spent catalysts.

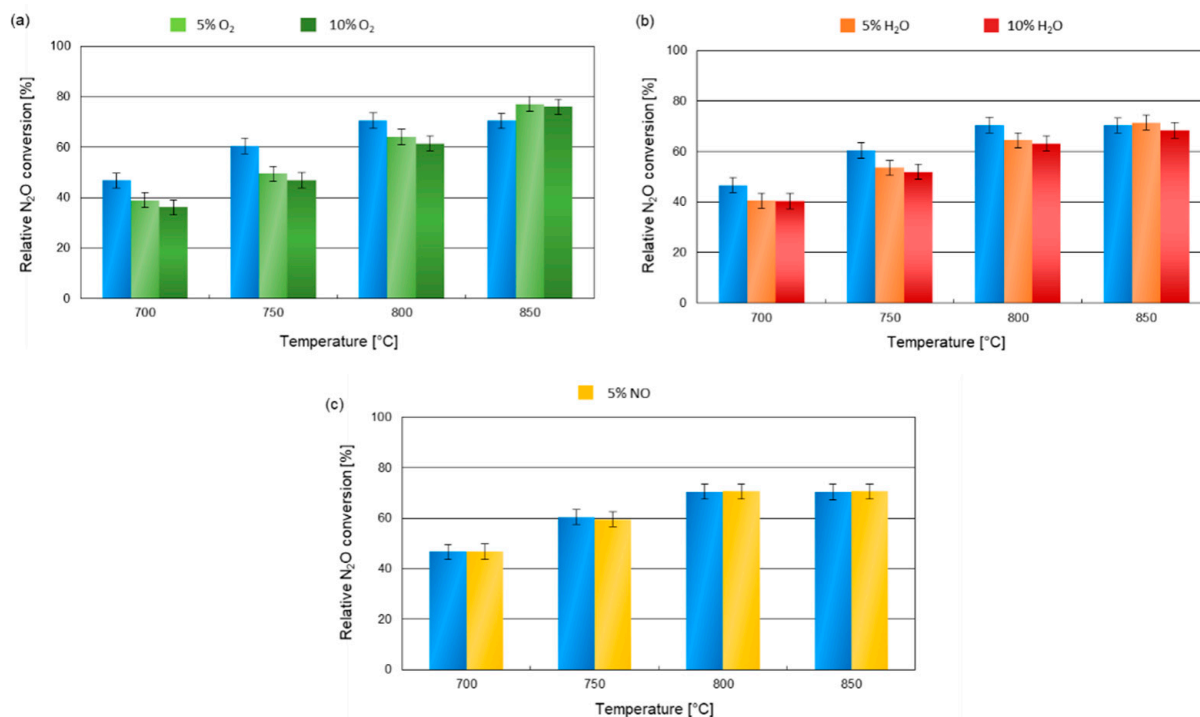


Figure 6. Nitrous oxide conversions in streams with different compositions: (a) 5 and 10 % O_2 concentration, 5% N_2O , Ar (b) 5 and 10% water vapor content, 5% N_2O , Ar and (c) 5% N_2O , Ar with and without 5% NO in the stream.

Figure 7 shows the diffraction patterns obtained from the two samples of $\text{Co}_{3.5}\text{La}$ after operating at 850 °C in two streams, namely: 5 vol % N_2O + 5 vol % O_2 in Ar and 5 vol % N_2O in Ar, respectively. It can be seen that the sample operating in a mixture containing 5 vol % oxygen has cobalt mostly in the form of Co_3O_4 , whereas the one operating without an addition of oxygen has cobalt present mostly as CoO . These findings correspond to the results obtained for the undoped cobalt catalyst operating in mixtures with these compositions [37]. Comparing these data with those from XPS measurements (Figure 5 spectrum 3) and the ones obtained previously for the undoped cobalt catalyst, it is interesting that, although LaCoO_3 does not lead to a higher degree of oxidation of cobalt in the catalyst, the activity of $\text{Co}_{3.5}\text{La}$ is so high even without the addition of oxygen to the inlet stream. Moreover, the positive effect of the addition of oxygen to the feed at 850 °C is much less pronounced than in the undoped cobalt catalyst. When considering a possible reason for this difference, it should be taken into account that a certain amount of oxygen is always present in the reaction mixture as it is one of the products of N_2O decomposition.

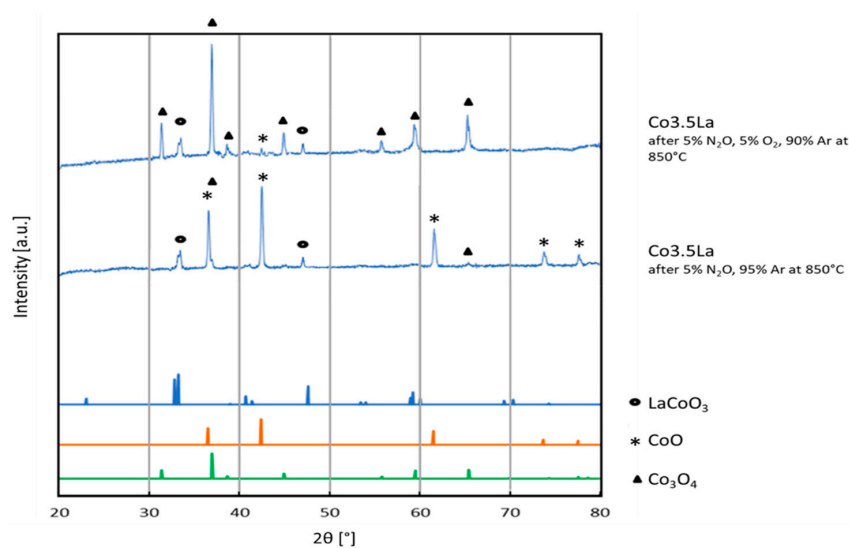


Figure 7. The diffraction patterns of Co_{3.5}La obtained from a sample operating at 850 °C in 5%N₂O + 95%Ar and in a 5%N₂O + 5%O₂ + 90%Ar mixture, along with the appropriate reference patterns of Co₃O₄ (71-0816)—triangles and CoO (48-1719)—stars.

The influence of the presence of water vapor in the inlet stream on the nitrous oxide conversion on Co_{3.5}La is shown in Figure 6b. As can be seen, the addition of 5 vol % water vapor to the reactant mixture reduces the activity to a certain extent in the entire investigated temperature range, except at 850 °C, at which the conversion is the same with or without the addition of water vapor. A further increase of the H₂O(g) concentration has no effect on the N₂O conversion.

The addition of 5 vol % of the nitric oxide to the inlet stream does not affect the degree of conversion of nitrous oxide under the tested conditions (Figure 6c). The N₂O conversion on Co_{3.5}La is the same in the stream with the initial composition 5 vol % N₂O + 5 vol % NO in Ar and 5 vol % N₂O in Ar. In the case of the undoped cobalt catalyst, the presence of NO in the stream led to higher levels of conversion of nitrous oxide at the temperature of 850 °C. It is known from literature that the rate limiting step for N₂O decomposition is the formation of molecular oxygen from two anions deposited on the surface by two molecules of N₂O, i.e., desorption of O₂ from the surface of the catalyst [6]. Nitric oxide is known for its "scavenger" properties, which enables the transport of oxygen anions away from the surface. A pronounced positive effect was observed on Cu-zeolites especially when the distance between Cu cations was increased [41]. Therefore, the same conversions obtained in the presence of Co_{3.5}La in the mixture without and with NO provide evidence of the positive impact of LaCoO₃. A positive effect of doping Co₃O₄-based catalysts with either ceria [5] or cesium [27] has been attributed to the shortening of the Co-O bond and hence facilitation of the desorption of oxygen from the catalyst surface. It may be assumed that in the case of LaCoO₃ the positive effect is also caused by easier O₂ desorption. Since LaCoO₃ is known to exhibit high mobility of oxygen and an increased mobility of oxygen in the catalyst might affect the formation and desorption of molecular oxygen, the observed behavior may be due to an overall increased mobility of oxide anions. This would account for a negative effect of the increase in the concentration of oxygen in the reaction mixture, which causes an increased amount of oxygen anions occupying sites and making them unavailable to N₂O molecules. It would also explain why NO is not beneficial despite the fact that the majority of cobalt on the surface is present in the form of CoO. Thanks to the high oxygen mobility due to the presence of LaCoO₃, the catalyst would not need the "scavenger" to transport oxygen anions so that O₂ is desorbed as a molecule.

In order to validate the hypothesis that the reason for a positive effect of the LaCoO₃ perovskite on the activity of the Co_{3.5}La catalyst is facilitating the diffusion of oxygen ions throughout the entire catalytic system, a series of temperature-programmed oxidation

measurements was performed. TPO measurements were carried out after the reduction of the catalyst in hydrogen-rich stream. Then, the sample was oxidized in a reaction mixture with 5 vol % oxygen in an inert gas and the weight change resulting from the oxygen uptake was simultaneously monitored. Figure 8 shows the curves obtained in the tests as a function of time of the experiment. The dashed and dotted curve shows the temperature profile and refers to the right axis. The continuous curve shows the signal received during the oxidation of a sample of Co_{3.5}La whose weight was 0.475 g. The curve with long dashes refers to the sample of the undoped catalyst of the same weight. Cobalt oxidation occurs in two stages. Line 1 in Figure 8 marks the beginning of oxidation of Co_{3.5}La. It can be seen that at that temperature neither of the cobalt samples begins oxidation. The first step of cobalt oxidation is the oxidation of metal cobalt to CoO. Next, CoO is oxidized to Co₃O₄. In the presence of lanthanum, the oxidation begins at a lower temperature (Figure 8). The second step is particularly interesting in terms of this study, because under the conditions of the activity measurements both CoO and Co₃O₄ can be present, and the oxidation of CoO to Co₃O₄ is very important for the activity. The TPO results show a significant difference in the oxidation step for Co_{3.5}La and the undoped cobalt catalyst. The beginning of oxidation in Co_{3.5}La is marked with line 1. It can be seen that the undoped cobalt catalyst has not begun to oxidize. What is more, in the case of Co_{3.5}La the oxidation does not slow down, as it does in the undoped cobalt catalyst. The undoped cobalt catalyst finishes oxidation only during the isothermal segment, which starts at line 2. In order to verify whether this effect is not due to a slightly larger content of cobalt in the sample of the undoped catalyst and, therefore, to a larger demand for oxygen, another measurement was performed with less than half of this quantity, i.e., 0.210 g, of the undoped cobalt catalyst. The curve obtained during this measurement can be seen in Figure 8 as the line with short dashes. Although the amount of cobalt in this sample is considerably smaller than that in the Co_{3.5}La sample, the second stage of oxidation slows down and ends after the isothermal step started (Figure 8, line 2).

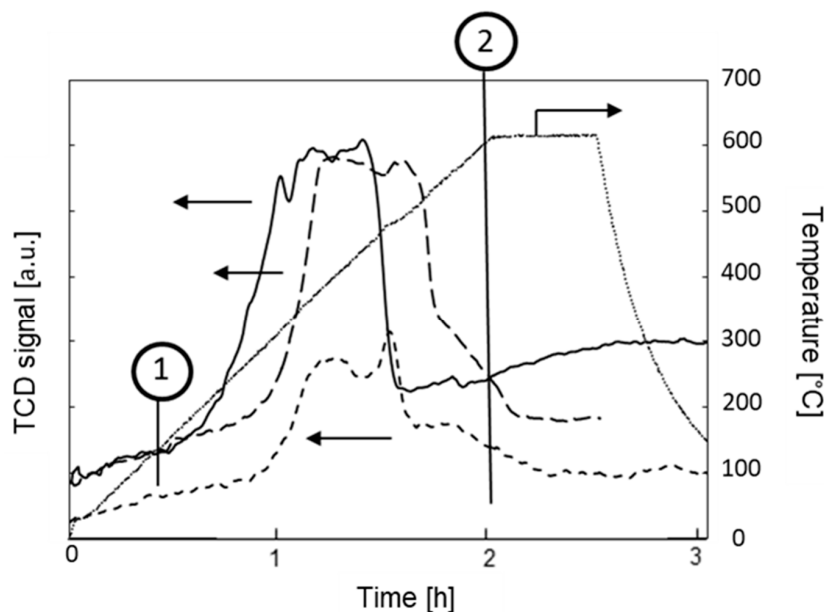


Figure 8. Temperature Programmed Oxidation (TPO) results of the undoped cobalt catalyst (long dashes: 475 mg; short dashes: 210 mg) and Co_{3.5}La (solid line: 475 mg) and the function of temperature in time (dotted line); line 1 indicates the onset of oxidation of Co_{3.5}La, line 2 indicates the beginning of the isothermal segment.

3. Materials and Methods

3.1. Catalyst Preparation

The catalyst was obtained from Co₃O₄ (POCH, Gliwice, Poland, pure) and lanthanum nitrate. In order to obtain lanthanum nitrate, lanthanum oxide (Fluka, St. Gallen, Switzer-

land, pure) was calcined at 800 °C for 12 h, cooled and dissolved in a 1:1 aqueous solution of nitric acid (POCH, Gliwice, Poland, 65% pure for analysis). Cobalt oxide was added to the solution. The resulting mixture was heated to approximately 800 °C for 3 h until lanthanum nitrate decomposed. Next, the mixture was heated in static air for approximately 16 h at 850 °C to allow for the reaction between Co_3O_4 and the even distribution of La_2O_3 (see Figure 1). The obtained solid was ground. For every 20.0 g of powder 1.0 g of ammonium carbonate (Riedel-de Haen, Seelze, Germany, pure) was added along with 0.3 g of glycerin (POCH, Gliwice, Poland, pure for analysis) in order to facilitate the formation of pellets. Both compounds decomposed entirely when the pellets were heated to 850 °C. The mixture was ground until it was homogeneous. Tablets (diameter 1.70 cm, height 0.3 cm) were pressed from the fraction below 0.4 mm. The force applied in two subsequent steps was 5 and 10 tons, respectively. Next, the tablets were calcined at 850 °C for 48 h, cooled, crushed and sieved.

3.2. Activity Measurements and Characterization Studies

The activity measurements were performed in a flow reactor with a quartz glass fixed bed of catalyst (0.5 mL, fraction size: 2.0–2.5 mm, $S_{\text{BET}} < 2 \text{ m}^2/\text{g}$). The experiments were conducted at four temperatures (700, 750, 800 and 850 °C) and the Gas Hourly Space Velocity (GHSV) was $1.2 \cdot 10^5 \text{ h}^{-1}$. The following gases were passed through the reactor: N_2O (Zach-Ciech, Bydgoszcz, Poland, medical grade), O_2 (Multax, Andover, UK, N5.0), NO (Linde Gas, Dublin, Ireland, N2.5), Ar (Multax, Andover, UK, N5.0) and water vapor, which was obtained in an evaporator from distilled water. The reaction mixture was fed through the bed from above. The degree of decomposition of nitrous oxide was measured for mixtures with the inlet stream having the following compositions: argon and N_2O (2.5 vol %, 5 vol % or 10 vol %); 5 vol % N_2O and O_2 (5 vol % or 10 vol %), 5 vol % N_2O and H_2O (5 vol % or 10 vol %); as well as 5 vol % N_2O and 5 vol % NO . The concentration of N_2O in these studies was significantly higher than that currently found directly downstream of the platinum gauze (300–3000 ppm [4]) in order to make certain that the lack of a difference is not the result of the experimental error, but an actual fact. A gas chromatograph (HRGC 4000B KONIK, Barcelona, Spain) with a TC detector and a column packed with PorapakQ was used to find the areas of the N_2O signals from samples of the inlet and outlet streams. The volume of N_2O in a sample was determined from the peak area and a calibration curve obtained from measurements with known amounts of N_2O injected onto the column. The conversion of nitrous oxide was calculated based on the following equation:

$$x = 100\% \cdot (V_{\text{in}} \cdot V_{\text{SYR}} - V_{\text{out}} \cdot V_{\text{SYR}}) / (V_{\text{SYR}} \cdot V_{\text{in}} + 0.5 \cdot V_{\text{in}} \cdot V_{\text{out}}) \quad (2)$$

where: x —conversion of N_2O [%]

V_{in} —volume of N_2O in syringe with inlet stream sample [μL],

V_{SYR} —volume of syringe [μL],

V_{out} —volume of N_2O in syringe with sample at outlet [μL].

The results are the average of six measurements, in which the values did not differ by more than 3%. The measurements were performed from the lowest temperature to the highest on one day and starting from the highest temperature to the lowest on the next day to ensure that the sequence of temperatures would not affect the results. In the case of the nitrous oxide conversions on $\text{Co}_3.5\text{La}$, the numbers were related to the slightly smaller amount of Co_3O_4 in the fresh catalyst than in the undoped cobalt catalyst.

The surface area and pore distribution of the undoped cobalt catalyst and $\text{Co}_3.5\text{La}$ (both fresh and after activity tests) were determined by nitrogen physisorption (ASAP 2020, Micromeritics). The area was calculated by applying the BET equation. The pore distribution was determined by the BJH method.

The phase composition and average size of the particles of each phase in the catalyst was established on the basis of the diffraction patterns. The measurement was performed using a Siemens D 5000 diffractometer (Bruker AXS GmbH, Karlsruhe, Germany) with a Cu sealed tube operated at a voltage of 40 kV and a current of 40 mA. The measurement

was performed at 2θ angular range from 5° to 100° in steps of 0.2° at a rate of 1.0 s step^{-1} . The average particle size was calculated using the Sherrer equation.

The diffraction patterns for samples after activity measurements were obtained from quenched samples which operated at 850°C in two inlet streams, namely: 5 vol % O_2 + 5 vol % N_2O in Ar and in 5 vol % N_2O in Ar, for 4 h.

XPS measurements of samples of the fresh catalyst and of samples after operating in a stream of 5 vol % N_2O in Ar and 5 vol % O_2 + 5 vol % N_2O in Ar were performed with a scanning photoelectron spectrometer PHI 5000 VersaProbe (Physical Electronics ULVAC, Chesham, UK). A monochromatic beam anode was used for the measurement. The beam of Al $K\alpha$ radiation with the energy of 1486.6 eV was focused on a $100 \cdot 100 \mu\text{m}$ surface. The beam power was 25 W and the voltage was 15 kV. The analyzer and the radiation source were set at 45° to the analyzed surface. The survey spectra were collected with pass energy of 117.4 eV, with a measuring step 0.4 eV. High-resolution scans of the following regions: Co 2p, O 1s, C 1s and La 3d, were obtained with pass energy of 23.5 eV and a step of 0.1 eV.

Secondary Electron Microscopy images were obtained using a Quanta FEG 250 instrument (Field Electron and Ion Company, FEI, Hillsboro, OR, USA). The measurements were carried with the following parameters: working distance (WD) approx. 8 mm, beam energy: 20 kV, magnification: 2000 times.

Temperature programmed oxidation experiments were performed in a flow system in a quartz glass reactor using a PEAK 4 instrument (Łódź University of Technology, Łódź, Poland) equipped with a thermal conductivity detector. The following gases were used: hydrogen (N5.0, Air Products, Allentown, PA, USA), oxygen (N5.0, Multax, Andover, UK) and the carrier gas, helium (N5.0, Multax, Andover, UK), with a total flow of 40 mL min^{-1} . Helium was additionally purified so that after the reduction of all oxygen-containing species no more than 0.5 ppm of water vapor was present. The experiments were performed by placing a weighed sample of a catalyst (0.475 g of $\text{Co}_{3.5}\text{La}$ and 0.475 g or 0.210 g of the undoped cobalt catalyst; grain size 0.4–1.0 mm) and reducing the sample at 600°C in a gas stream containing 80 vol % H_2 in helium for 15 h. Next, the sample was held in a He stream for 30 min; $T = 600^\circ\text{C}$, then cooled to 30°C in a He stream. After the calibration of the TCD, the sample was heated to 600°C at a rate of 5°C min^{-1} in a mixture containing 5 vol % oxygen and the temperature was maintained for an additional 30 min.

4. Conclusions

The activity tests showed that the preparation method yielded in successfully obtaining a catalyst which contains Co_3O_4 and LaCoO_3 . In this catalyst, a substantial thermal reduction of Co_3O_4 to CoO did not lead to a drop of activity in N_2O conversion. The reason for this was better understood based on the results with different inlet stream compositions.

It was found that the addition of oxygen to the inlet stream does not have a substantial positive effect, whereas the addition of water vapor does not have a significant negative effect on the activity of the new catalyst. Moreover, the addition of NO, an “oxygen scavenger” [37], did not affect the performance of $\text{Co}_{3.5}\text{La}$. This suggests an efficient oxygen removal from the surface of the $\text{Co}_{3.5}\text{La}$ catalyst.

The results of TPO tests clearly show that the presence of a small amount of lanthanum cobaltate has a beneficial effect on the rate of oxidation of cobalt, which is likely due to the increased migration of oxygen ions through the cobalt oxides formed during the experiment. The impact of LaCoO_3 on the activity of the catalyst was therefore attributed to the increased mobility of oxygen, which facilitates the desorption of oxygen from the surface. This also accounts for the lack of beneficial effect of the addition of an “oxygen scavenger”, NO, on the activity of $\text{Co}_{3.5}\text{La}$.

Author Contributions: Conceptualization, J.P., E.M.I. and L.F.L.; formal analysis, J.P., E.M.I., Z.K., J.W.S. and L.F.L.; investigation, L.F.L., G.P., J.W.S., E.M.I. and E.G.; resources, J.P.; data curation, E.M.I., Z.K., L.F.L. and G.P.; writing—original draft preparation, E.M.I.; writing—review and editing,

L.F.L., J.P. and K.K.; visualization, E.M.I. and Z.K.; project administration, J.P., E.M.I., K.K. and L.F.L.; funding acquisition, J.P. All authors have read and agreed to the published version of the manuscript.

Funding: These studies were funded by the Ministry of Science and Higher Education of Poland, within the Research Project NN205 012434.

Acknowledgments: The authors express gratitude to Ilya Gourevich from the Centre for Nanostructure Imaging (CNI) at the University of Toronto, Canada, for conducting the SEM-EDX measurements.

Conflicts of Interest: The authors declare no conflict of interest.

References

1. Cole, K.M.; Kirk, D.W.; Thorpe, S.J. Co_3O_4 nanoparticles characterized by XPS and UPS. *Surf. Sci. Spectra* **2021**, *28*, 014001. [[CrossRef](#)]
2. Peck, T.C.; Roberts, C.A.; Reddy, G.K. Contrasting Effects of Potassium Addition on M_3O_4 ($\text{M} = \text{Co}, \text{Fe}, \text{and Mn}$) Oxides during Direct NO Decomposition Catalysis. *Catalysts* **2020**, *10*, 561. [[CrossRef](#)]
3. Wójcik, S.; Grzybek, G.; Stelmachowski, P.; Sojka, Z.; Kotarba, A. Bulk, Surface and Interface Promotion of Co_3O_4 for the Low-Temperature N_2O Decomposition Catalysis. *Catalysts* **2020**, *10*, 41. [[CrossRef](#)]
4. Liotta, L.F.; Ousmane, M.; Di Carlo, G.; Pantaleo, G.; Deganello, G.; Marcic, G.; Retailleau, L.; Giroir-Fendler, A. Total oxidation of propene at low temperature over Co_3O_4 - CeO_2 mixed oxides: Role of surface oxygen vacancies and bulk oxygen mobility in the catalytic activity. *Appl. Catal. A* **2008**, *34*, 781–788. [[CrossRef](#)]
5. Iwanek, E.; Krawczyk, K.; Petryk, J.; Sobczak, J.W.; Kaszukur, Z. Direct nitrous oxide decomposition with CoO_x - CeO_2 catalysts. *Appl. Catal. B* **2011**, *106*, 416–422. [[CrossRef](#)]
6. Kapteijn, F.; Rodriguez-Mirasol, J.; Moulijn, J.A. Heterogeneous catalytic decomposition of nitrous oxide. *Appl. Catal. B* **1996**, *9*, 25–64. [[CrossRef](#)]
7. Darda, S.; Pachatouridou, E.; Lappas, A.; Iliopoulou, E. Effect of Preparation Method of Co-Ce Catalysts on CH_4 Combustion. *Catalysts* **2019**, *9*, 219. [[CrossRef](#)]
8. Liotta, L.; Di Carlo, G.; Pantaleo, G.; Venezia, A.; Deganello, G. Co_3O_4 / CeO_2 composite oxides for methane emissions abatement: Relationship between Co_3O_4 - CeO_2 interaction and catalytic activity. *Appl. Catal. B Environ.* **2006**, *66*, 217–227. [[CrossRef](#)]
9. Konsolakis, M.; Sgourakis, M.; Carabineiro, S.A. Surface and redox properties of cobalt-ceria binary oxides: On the effect of Co content and pretreatment conditions. *Appl. Surf. Sci.* **2015**, *341*, 48–54. [[CrossRef](#)]
10. Simonot, L.; Garin, F.; Maire, G. A comparative study of LaCoO_3 , Co_3O_4 and LaCoO_3 - Co_3O_4 : I. Preparation, characterisation and catalytic properties for the oxidation of CO. *Appl. Catal. B Environ.* **1997**, *11*, 167–179. [[CrossRef](#)]
11. Liotta, L.; Di Carlo, G.; Longo, A.; Pantaleo, G.; Deganello, G.; Marci, G.; Martorana, A. Structural and morphological properties of Co-La catalysts supported on alumina/lanthana for hydrocarbon oxidation. *J. Non-Cryst. Solids* **2004**, *345*, 620–623. [[CrossRef](#)]
12. Liu, S.; Zhang, W.; Deng, T.; Wang, D.; Wang, X.; Zhang, X.; Zhang, C.; Zheng, W. Mechanistic Origin of Enhanced CO Catalytic Oxidation over Co_3O_4 / LaCoO_3 at Lower Temperature. *ChemCatChem* **2017**, *9*, 3102–3106. [[CrossRef](#)]
13. Abadian, L.; Malekzadeh, A.; Khodadadi, A.A.; Mortazavi, Y. Effects of Excess Cobalt Oxide Nanocrystallites on LaCoO_3 Catalyst on Lowering the Light off Temperature of CO and Hydrocarbons Oxidation. *Iran. J. Chem. Chem. Eng.* **2008**, *27*, 71–77.
14. Atkinson, A. Chemically-induced stresses in gadolinium-doped ceria solid oxide fuel cell electrolytes. *Solid State Ionics* **1997**, *95*, 249–258. [[CrossRef](#)]
15. Lee, J.G.; Park, J.H.; Shul, Y.G. Tailoring gadolinium-doped ceria-based solid oxide fuel cells to achieve 2 W cm^{-2} at $550 \text{ }^\circ\text{C}$. *Nat. Commun.* **2014**, *5*, 4045. [[CrossRef](#)] [[PubMed](#)]
16. Fuentes, R.; Baker, R. Synthesis and properties of Gadolinium-doped ceria solid solutions for IT-SOFC electrolytes. *Int. J. Hydrog. Energy* **2008**, *33*, 3480–3484. [[CrossRef](#)]
17. Hussain, S.; Yangping, L. Review of solid oxide fuel cell materials: Cathode, anode, and electrolyte. *Energy Transit.* **2020**, *4*, 113–126. [[CrossRef](#)]
18. Rehman, S.U.; Song, R.-H.; Lim, T.-H.; Park, S.-J.; Hong, J.-E.; Lee, J.-W.; Lee, S.-B. High-performance nanofibrous LaCoO_3 perovskite cathode for solid oxide fuel cells fabricated via chemically assisted electrodeposition. *J. Mater. Chem. A* **2018**, *6*, 6987–6996. [[CrossRef](#)]
19. Ivers-Tiffée, E.L.; Weber, A.; Herbstritt, D. Materials and technologies for SOFC-components. *J. Eur. Ceram. Soc.* **2001**, *21*, 1805–1811. [[CrossRef](#)]
20. Mihara, S.; Kobayashi, K.; Akashi, T.; Sakka, Y. Chemical Reactivity and Cathode Properties of LaCoO_3 on Lanthanum Silicate Oxyapatite Electrolyte. *Key Eng. Mater.* **2014**, *616*, 120–128. [[CrossRef](#)]
21. Khalil, M.S. Synthesis, X-ray, infrared spectra and electrical conductivity of La/Ba- CoO_3 systems. *Mater. Sci. Eng. A* **2003**, *352*, 64–70. [[CrossRef](#)]
22. Wang, C.; Xiao, M.; Hu, J.; Ling, C.; Zhang, C.; Lan, J.; Hui, Y.; Liu, D. Conductivity and Infrared Absorption of $\text{La}_{1-x}\text{Ba}_x\text{CoO}_3$ Conductive Ceramics. *J. Solid State Chem.* **1998**, *137*, 211–213. [[CrossRef](#)]
23. Shuk, P.; Charton, V.; Samochval, V. Mixed Conductors on the Lanthanid Cobaltites Basis. *Mater. Sci. Forum* **1991**, *76*, 161–164. [[CrossRef](#)]

24. Tišler, Z.; Klegová, A.; Svobodová, E.; Šafář, J.; Strejcová, K.; Kohout, J.; Šlang, S.; Pacultová, K.; Rodríguez-Padrón, D.; Bulánek, R. Cobalt Based Catalysts on Alkali-Activated Zeolite Foams for N₂O Decomposition. *Catalysts* **2020**, *10*, 1398. [[CrossRef](#)]
25. Inger, M.; Moszowski, B.; Ruzsak, M.; Rajewski, J.; Wilk, M. Two-Stage Catalytic Abatement of N₂O Emission in Nitric Acid Plants. *Catalysts* **2020**, *10*, 987. [[CrossRef](#)]
26. Karásková, K.; Pacultová, K.; Jirátová, K.; Fridrichová, D.; Koštejn, M.; Obalová, L. K-Modified Co–Mn–Al Mixed Oxide—Effect of Calcination Temperature on N₂O Conversion in the Presence of H₂O and NO_x. *Catalysts* **2020**, *10*, 1134. [[CrossRef](#)]
27. Bernauer, M.; Bernauer, B.; Sádovská, G.; Sobalík, Z. High-temperature decomposition of N₂O from the HNO₃ production: Process feasibility using a structured catalyst. *Chem. Eng. Sci.* **2020**, *220*, 115624. [[CrossRef](#)]
28. Pasha, N.; Lingaiah, N.; Babu, N.S.; Reddy, P.S.S.; Prasad, P.S. Studies on cesium doped cobalt oxide catalysts for direct N₂O decomposition in the presence of oxygen and steam. *Catal. Commun.* **2008**, *10*, 132–136. [[CrossRef](#)]
29. Armor, J.; Braymer, T.; Farris, T.; Li, Y.; Petrocelli, F.; Weist, E.; Kannan, S.; Swamy, C. Calcined hydrotalcites for the catalytic decomposition of N₂O in simulated process streams. *Appl. Catal. B* **1996**, *7*, 397–406. [[CrossRef](#)]
30. Centi, G.; Cerrato, G.; D'Angelo, S.; Finardi, U.; Giamello, E.; Morterra, M.; Perathoner, S. Reactivity, Stability and Characterization of Cu-ZrO₂ Catalysts for the Decomposition of N₂O in Industrial Effluents. In Proceedings of the Environmental Catalysis: 1st World Conference, Pisa, Italy, 1–5 May 1995; pp. 175–178.
31. Centi, G.; Galli, A.; Montanari, B.; Perathoner, S.; Vaccaria, A. Catalytic decomposition of N₂O over noble and transition metal containing oxides and zeolites. Role of some variables on reactivity. *Catal. Today* **1997**, *35*, 113–120. [[CrossRef](#)]
32. Marnellos, G.E.; Efthimiadis, E.A.; Vasalos, I.A. Effect of SO₂ and H₂O on the N₂O decomposition in the presence of O₂ over Ru/Al₂O₃. *Appl. Catal. B* **2003**, *46*, 523–539. [[CrossRef](#)]
33. Oi, J.; Obuchi, A.; Bamwenda, G.R.; Ogata, A.; Yagita, H.; Kushiyama, S.; Mizuno, K. Decomposition of nitrous oxide over supported rhodium catalysts and dependency on feed gas composition. *Appl. Catal. B* **1997**, *12*, 277–286. [[CrossRef](#)]
34. Kapteijn, F.; Marbán, G.; Rodríguez-Mirasol, J.; Moulijn, J.A. Kinetic Analysis of the Decomposition of Nitrous Oxide over ZSM-5 Catalysts. *J. Catal.* **1997**, *167*, 256–265. [[CrossRef](#)]
35. Kögel, M.; Abu-Zied, B.M.; Schwefer, M.; Turek, T. The effect of NO_x on the catalytic decomposition of nitrous oxide over Fe-MFI zeolites. *Catal. Commun.* **2001**, *2*, 273–276. [[CrossRef](#)]
36. Tejuca, L.G.; Fierro, J.L.G.; Tascón, J.M. Structure and Reactivity of Perovskite-Type Oxides. *Adv. Catal.* **1989**, *36*, 237–328. [[CrossRef](#)]
37. Wilczkowska, E.; Krawczyk, K.; Petryk, J.; Sobczak, J.W.; Kaszukur, Z. Direct nitrous oxide decomposition with a cobalt oxide catalyst. *Appl. Catal. A* **2010**, *389*, 165–172. [[CrossRef](#)]
38. Giecko, G.; Borowiecki, T.; Gac, W.; Kruk, J. Fe₂O₃/Al₂O₃ catalysts for the N₂O decomposition in the nitric acid industry. *Catal. Today* **2008**, *137*, 403–409. [[CrossRef](#)]
39. Shen, Q.; Li, L.; Li, J.; Tian, H.; Hao, Z. A study on N₂O catalytic decomposition over Co/MgO catalysts. *J. Hazard. Mater.* **2009**, *163*, 1332–1337. [[CrossRef](#)]
40. Xue, L.; Zhang, C.; He, H.; Teraoka, Y. Catalytic decomposition of N₂O over CeO₂ promoted Co₃O₄ spinel catalyst. *Appl. Catal. B* **2007**, *75*, 167–174. [[CrossRef](#)]
41. Smeets, P.J.; Sels, B.F.; Van Teeffelen, R.M.; Leeman, H.; Hensen, E.J.M.; Schoonheydt, R.A. The catalytic performance of Cu-containing zeolites in N₂O decomposition and the influence of O₂, NO and H₂O on recombination of oxygen. *J. Catal.* **2008**, *256*, 183–191. [[CrossRef](#)]
42. Sang, C.; Lund, C.R. Possible role of nitrite/nitrate redox cycles in N₂O decomposition and light-off over Fe-ZSM-5. *Catal. Lett.* **2001**, *73*, 73–77. [[CrossRef](#)]
43. Mul, G.; Perez-Ramirez, J.; Kapteijn, F.; Moulijn, J.A. NO-Assisted N₂O Decomposition over ex-Framework FeZSM-5: Mechanistic Aspects. *Catal. Lett.* **2001**, *77*, 7–13. [[CrossRef](#)]
44. Xie, X.; Li, Y.; Liu, Z.-Q.; Haruta, M.; Shen, W. Low-temperature oxidation of CO catalysed by Co₃O₄ anorods. *Nature* **2009**, *458*, 746. [[CrossRef](#)] [[PubMed](#)]
45. Asano, K.; Ohnishi, C.; Iwamoto, S.; Shioya, Y.; Inoue, M. Potassium-doped Co₃O₄ catalyst for direct decomposition of N₂O. *Appl. Catal. B* **2008**, *78*, 242–249. [[CrossRef](#)]
46. Wilczkowska, E.; Kowalczyk, Z.; Petryk, J.; Raróg-Pilecka, W.; Kaszukur, Z. Catalytic Decomposition of Nitrous Oxide. *Pol. J. Chem.* **2009**, *83*, 515–518.
47. Barreca, D.; Massignam, C. Composition and Microstructure of Cobalt Oxide Thin Films Obtained from a Novel Cobalt(II) Precursor by Chemical Vapor Deposition. *Chem. Mater.* **2001**, *13*, 588–593. [[CrossRef](#)]
48. Petitto, S.C.; Marsh, E.M.; Carson, G.A.; Langell, M.A. Cobalt oxide surface chemistry: The interaction of CoO(100), Co₃O₄(110) and Co₃O₄(111) with oxygen and water. *J. Mol. Catal. A* **2008**, *281*, 49–58. [[CrossRef](#)]
49. Chuang, T.; Brundle, C.; Rice, D. Interpretation of the x-ray photoemission spectra of cobalt oxides and cobalt oxide surfaces. *Surf. Sci.* **1976**, *59*, 413–429. [[CrossRef](#)]